effect on the magnitude of the coupling between the iron centers. The most pronounced angle dependence is observed in the visible spectra of these complexes; our studies suggest that many of these features are dominated by oxo-to-Fe(III) charge-transfer bands. These observations provide us with a better understanding of the spectral features found for ($\mu$-oxo)diiron(III) centers in proteins.

**Acknowledgment.** We thank Professor J. D. Britton for his assistance and expertise with the structure determinations. This work was supported by grants from the National Institutes of Health (Grant No. GM-38767 to L.Q.) and the Louisiana Education Quality Support, administered by the Board of Regents of the State of Louisiana, and by the donors of the Petroleum Research Fund, administered by the American Chemical Society (C.J.O.). R.C.H. is grateful for a NIH postdoctoral fellowship (Grant GM-13919).

**Supplementary Material Available:** Ligand numbering scheme (Figure S1), tables of crystallographic parameters (Table S1), fractional atomic coordinates and isotropic thermal parameters (Tables S2-S4), bond lengths and angles (Tables S5-S7), and anisotropic thermal parameters (Tables S8-S10) for **1**, **4**, and **9**, and fits of the susceptibility data (Figures S2-S5) for **1**, **5**, **9**, and **10** (80 pages). Ordering information is given on any current masthead page.

---

Contribution from the Department of Chemistry,
Texas A&M University, College Station, Texas 77843

# Solid-State and Solution Structure of $(bpy)CuCo(CO)_4$ (bpy = 2,2′-Bipyridine)

Donald J. Darensbourg,* Chi-Shan Chao, Christopher Bischoff, and Joseph H. Reibenspies

*Received January 16, 1990*

The heterobimetallic complex $(bpy)CuCo(CO)_4$ has been prepared by the reaction of $NaCo(CO)_4$ with 2,2′-bipyridine and CuCl in dichloromethane and has been characterized by X-ray crystallography at −80 °C. The complex crystallizes in the monoclinic space group $P2_1/a$, with unit cell dimensions $a$ = 7.210 (3) Å, $b$ = 16.580 (6) Å, $c$ = 11.912 (6) Å, $\beta$ = 97.88 (4)°, $V$ = 1410 (1) Å$^3$, $Z$ = 4, and $R_F$ = 3.34%. The Cu–Co bond distance was found to be 2.404 (1) Å and to be supported by an asymmetrically bridged carbonyl ligand. This bridging CO group persists in polar solvents as well, as indicated by a $\nu$(CO) band at 1850 cm$^{-1}$ in the infrared spectra in both THF and Nujol mull. On the other hand, the Cu–Co bond is disrupted by a facile reaction at −78 °C with dppe (1,2-bis(diphenylphosphino)ethane) to provide the $Co(CO)_4^-$ anion and $Cu(bpy)(dppe)^+$.

## Introduction

Although heterobimetallic complexes with transition metal to copper bonds are uncommon, the syntheses of dinuclear copper–cobalt derivatives originating from the reaction of the $Co(CO)_4^-$ anion and copper(I) salts have received some attention.[1,2] Because of the variety of CO bonding modes open in these derivatives, in particular the presence of semibridging carbonyls, it is of importance to assess their structures both in the solid state via X-ray crystallography and in solution by spectroscopic techniques. Indeed, the electronic structure and bonding in the derivative that has been structurally characterized, namely $(tmed)CuCo(CO)_4$ (tmed = tetramethylethylenediamine), have been described on the basis of Fenske–Hall molecular orbital computations.[3]

In relation to the studies indicated above, we have recently reported the synthesis and structure of $[Cu(dmpe)_2][Cu(Co(CO)_4)_2]$, a complex containing copper(I) linearly bonded to two $Co(CO)_4^-$ anions.[4] Indeed, this latter complex was prepared in a manner completely analogous to that employed in the preparation of $(tmed)CuCo(CO)_4$ (eqs 1 and 2). At this time we wish

$$\mathrm{CuCl + dmpe + NaCo(CO)_4 \rightarrow \tfrac{1}{2}[Cu(dmpe)_2][Cu(Co(CO)_4)_2] + NaCl} \quad (1)$$

$$\mathrm{CuCl + tmed + NaCo(CO)_4 \rightarrow (tmed)CuCo(CO)_4 + NaCl} \quad (2)$$

to describe the solid-state and solution structure of $(bpy)CuCo(CO)_4$. This particular derivative was chosen for our investigation because it along with its 1,10-phenanthroline analogue had been suggested, on the basis of a complicated solid-state infrared spectrum, to contain a metal–carbonyl anion. Hence, it too might be formulated as $[Cu(bpy)_2][Cu(Co(CO)_4)_2]$.

## Experimental Section

**Methods and Materials.** All manipulations were carried out either in an argon drybox or on a double-manifold Schlenk vacuum line, using freshly distilled solvents. Reagent grade tetrahydrofuran and hexane were purified by distillation under nitrogen from sodium benzophenone ketyl. Dichloromethane was refluxed under nitrogen over phosphorus pentoxide and distilled prior to use. CuCl and 2,2′-bipyridine (bpy) were purchased from Aldrich Chemical Co. $Co_2(CO)_8$ and 1,2-bis(diphenylphosphino)ethane (dppe) were obtained from Strem Chemical Inc. $NaCo(CO)_4$ was prepared from NaOH and $Co_2(CO)_8$ according to published procedures.[5] Infrared spectra were recorded on an IBM FTIR/32 spectrometer.

**Table I.** Crystallographic Data for $(bpy)CuCo(CO)_4$

| | | | |
|---|---|---|---|
| chem formula | $C_{14}H_8N_2O_4CoCu$ | $V$, Å$^3$ | 1410 (1) |
| fw | 390.7 | $Z$ | 4 |
| space group | $P2_1/a$ | $D_{calcd}$, g/cm$^3$ | 1.840 |
| $a$, Å | 7.210 (3) | $\mu$(Mo K$\alpha$), cm$^{-1}$ | 27.04 |
| $b$, Å | 16.580 (6) | $\lambda$, Å | 0.71073 |
| $c$, Å | 11.912 (6) | $R_F$, %$^a$ | 3.34 |
| $\beta$, deg | 97.88 (4) | $R_{wF}$, %$^a$ | 3.22 |

$^a$ $R_F = \sum|\Delta|/\sum|F_o|$ and $R_{wF} = \sum(|\Delta|w^{1/2})/\sum(|F_o|w^{1/2})$, where $\Delta = |F_o| - |F_c|$.

**Synthesis of $(bpy)CuCo(CO)_4$.** CuCl (0.51 g, 5.2 mmol) was placed in a 100-mL Schlenk flask in the drybox. Upon removal of the flask from the drybox and the addition of 40 mL of $CH_2Cl_2$ by way of syringe, bpy (0.81 g, 5.2 mmol) in 30 mL of $CH_2Cl_2$ was added via cannula to the solution under $N_2$. The reaction was then placed under a CO atmosphere for 30 min. Subsequent to the addition of $NaCo(CO)_4$ (1.0 g, 5.2 mmol), the solution was stirred for 2 h and then filtered under $N_2$ to remove NaCl. The filtrate was concentrated to ca. 10 mL, and 60 mL of hexane was added. The product precipitated as an orange-red powder (1.5 g, 75%) and was recrystallized from $CH_2Cl_2$/hexane. Anal. Calcd for ($C_{14}H_8N_2O_4CoCu$): C, 43.01; H, 2.05. Found: C, 43.00; H, 2.05. IR (THF): 2024 (m), 1947 (vs), 1932 (s, sh), 1850 (m) cm$^{-1}$. IR (Nujol mull): 2020 (m), 1937 (vs), 1926 (s, sh), 1850 (m) cm$^{-1}$.

**Reaction of $(bpy)CuCo(CO)_4$ with dppe.** The complex $(bpy)CuCo(CO)_4$ was reacted with 1 equiv of dppe in THF at −78 °C. The reaction was monitored by IR spectroscopy, and the final infrared spectrum revealed formation of $Co(CO)_4^-$. The reaction rate of $(bpy)CuCo(CO)_4$ with incoming nucleophiles was dependent on the concentration and the nature of the nucleophile; e.g., dppe was found to react faster than $PPh_3$.

**Reaction of $(bpy)CuCo(CO)_4$ with Water.** Deoxygenated water was added to a flask containing a solid sample of $(bpy)CuCo(CO)_4$ under

---

(1) Hackett, P.; Manning, A. R. *J. Chem. Soc., Dalton Trans.* **1975**, 1606.
(2) Doyle, G.; Eriksen, K. A.; Van Engen, D. *Organometallics* **1985**, *4*, 877.
(3) Sargent, A. L.; Hall, M. B. *J. Am. Chem. Soc.* **1989**, *111*, 1563.
(4) Darensbourg, D. J.; Chao, C. S.; Reibenspies, J. H.; Bischoff, C. J. *Inorg. Chem.* **1990**, *29*, 2153.
(5) Edgell, W. F.; Lyford, J., IV. *Inorg. Chem.* **1970**, *9*, 1932.

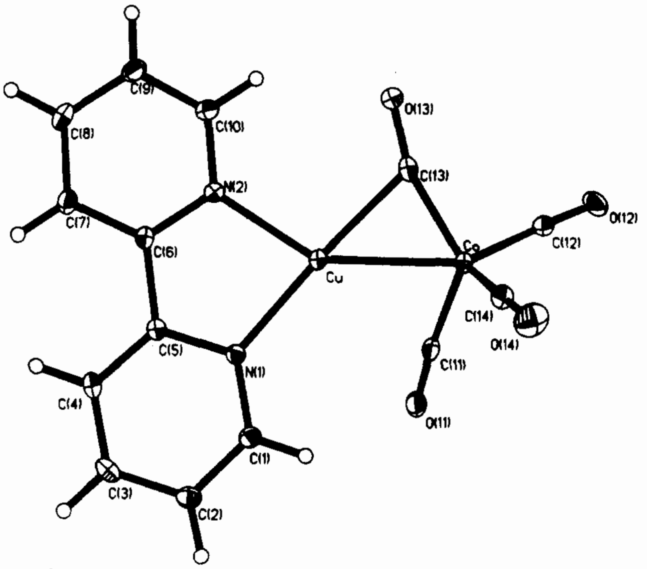

**Figure 1.** ORTEP diagram of (bpy)CuCo$(CO)_4$. Thermal ellipsoids are at 50% probability.

nitrogen, and the mixture was stirred for several minutes at ambient temperature. An infrared spectrum of the aqueous phase revealed no $Co(CO)_4^-$ in solution. The complex was quantitatively recovered upon removal of the water by decantation followed by vacuum drying.

**X-ray Crystallographic Study of (bpy)CuCo$(CO)_4$.** Crystal data and details of data collection are given in Table I. An orange needle (0.08 mm × 0.18 mm × 0.50 mm) was mounted on a glass fiber with vacuum grease at room temperature and cooled to −80 °C in a $N_2$ cold stream (Nicolet LT-2). Preliminary examination and data collection were performed on a Nicolet R3m/V X-ray diffractometer (oriented graphite monochromator; Mo K$\alpha$ $\lambda$ = 0.710 73 Å radiation). Cell parameters were calculated from the least-squares fitting of the setting angles for 25 reflections ($2\theta_{av}$ = 19.6°). $\omega$ scans for several intense reflections indicated good crystal quality. Data were collected for $4.0° \le 2\theta \le 50.0°$ [$\omega$-(Wyckoff) scans, $-8 \le h \le 8$, $0 \le k \le 19$, $0 \le l \le 14$] at 193 K. The scan range for the data collection was 1.20° plus K$\alpha$ separation, with a variable scan rate of 1.50–15.00° $min^{-1}$. Three control reflections, collected every 97 reflections, showed no significant trends. Background measurement was by the stationary-crystal/stationary-counter technique at the beginning and end of each scan for half of the total scan time. Lorentz and polarization corrections were applied to 2738 reflections. Extinction corrections were not applied. A semiempirical absorption correction was applied (ellipsoid approximation; $\mu$ = 0.05; $T_{max}$ = 0.9266, $T_{min}$ = 0.8232). A total of 2103 unique observed reflections ($R_{int} = \sum|F^2 - (F^2)_{mean}|/\sum F^2 = 0.01$), with $|I| \ge 1.3\sigma(I)$, were used in further calculations. The structure was solved by direct methods (SHELXS, SHELXTL-PLUS program package).[6] Full-matrix least-squares anisotropic refinement for all non-hydrogen atoms [SHELXLS, SHELXTL-PLUS program package; number of least-squares parameters = 199; quantity minimized $\sum w(F_o - F_c)^2$; $w = \sigma^2(F) + gF^2$; $g$ = 0.0001] yielded $R$ = 0.033, $R_w$ = 0.032, and $S$ = 1.61 at convergence (largest $\Delta/\sigma$ = 0.0035; mean $\Delta/\sigma$ = −0.0001; largest positive peak in the final Fourier difference map = 0.33 e $Å^3$; largest negative peak in the final Fourier difference map = −0.45 e $Å^3$). Hydrogen atoms were placed in idealized positions with isotropic thermal parameters fixed at 0.08. Neutral-atom scattering factors and anomalous dispersion terms were taken from the literature.[7] Tables listing observed and calculated structure factors are available as supplementary material.

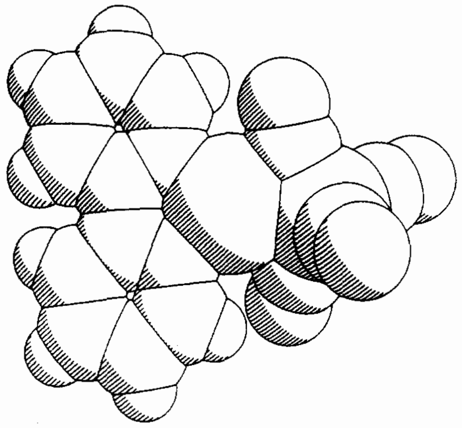

**Figure 2.** Space-filling diagram of (bpy)CuCo$(CO)_4$.

**Table II.** Atomic Coordinates ($\times 10^4$) and Equivalent Isotropic Displacement Parameters ($Å^2 \times 10^3$) for (bpy)CuCo$(CO)_4$

| | $x$ | $y$ | $z$ | $U$(eq)[a] |
|---|---|---|---|---|
| Cu | 2099 (1) | 1192 (1) | 7483 (1) | 28 (1) |
| Co | 2114 (1) | −258 (1) | 7512 (1) | 29 (1) |
| N(1) | 1057 (3) | 1972 (2) | 6223 (2) | 25 (1) |
| C(1) | 210 (4) | 1796 (2) | 5168 (3) | 30 (1) |
| C(2) | −426 (5) | 2378 (2) | 4377 (3) | 33 (1) |
| C(3) | −189 (5) | 3181 (2) | 4681 (3) | 34 (1) |
| C(4) | 663 (5) | 3373 (2) | 5757 (3) | 32 (1) |
| C(5) | 1276 (4) | 2762 (2) | 6511 (3) | 24 (1) |
| C(6) | 2207 (4) | 2915 (2) | 7690 (3) | 25 (1) |
| C(7) | 2483 (5) | 3691 (2) | 8131 (3) | 36 (1) |
| C(8) | 3373 (5) | 3781 (2) | 9231 (3) | 41 (1) |
| C(9) | 3931 (5) | 3105 (2) | 9865 (3) | 38 (1) |
| C(10) | 3602 (5) | 2358 (2) | 9374 (3) | 33 (1) |
| N(2) | 2754 (3) | 2256 (2) | 8306 (2) | 27 (1) |
| C(11) | 2462 (5) | −4 (2) | 6106 (3) | 34 (1) |
| O(11) | 2679 (4) | 108 (2) | 5179 (2) | 45 (1) |
| C(12) | 3536 (5) | −1118 (2) | 7876 (3) | 35 (1) |
| O(12) | 4398 (4) | −1686 (2) | 8102 (2) | 51 (1) |
| C(13) | 2743 (6) | 334 (2) | 8760 (3) | 39 (1) |
| O(13) | 3171 (5) | 522 (2) | 9704 (2) | 59 (1) |
| C(14) | −272 (5) | −557 (2) | 7485 (3) | 36 (1) |
| O(14) | −1766 (4) | −769 (2) | 7476 (2) | 59 (1) |

[a] Equivalent isotropic $U$ defined as one-third of the trace of the orthogonalized $U_{ij}$ tensor.

## Results

The reaction of CuCl with 2,2′-bipyridine in methylene chloride in the presence of NaCo$(CO)_4$, subsequent to concentration of the solution and addition of hexane, provided an orange-red powder in 75% yield. The resultant complex exhibited an elemental analysis consistent with its formulation as (bpy)CuCo$(CO)_4$. Furthermore, the infrared spectrum of the complex displayed four $\nu$(CO) frequencies in Nujol mull at 2020 (m), 1937 (vs), 1926 (s, sh), and 1850 (m) $cm^{-1}$, which are quite similar to those reported by Doyle for a similarly prepared complex, as well as for the structurally characterized (tmed)CuCo$(CO)_4$ derivative.[2] On the other hand Manning and co-workers[1] reported, in their preparation of the 2,2′-bipyridine complex, five $\nu$(CO) vibrational modes in Nujol mull at 2020, 1938, 1926, 1917, and 1857 $cm^{-1}$.

In order to define precisely the molecular structure of the complex prepared, it was subjected to a single-crystal X-ray diffraction investigation at −80 °C. Orange crystals suitable for X-ray structure analysis were obtained by slow diffusion of hexane into a concentrated methylene chloride solution of the compound at ambient temperature. An ORTEP view of the molecule is depicted in Figure 1, whereas a space-filling diagram of (bpy)CuCo$(CO)_4$ is shown in Figure 2. The final atomic coordinates for all non-hydrogen atoms are provided in Table II. Bond lengths and bond angles are listed in Table III.

## Discussion

The overall molecular geometry of the (bpy)CuCo$(CO)_4$ complex is quite similar to that of the previously reported structure of (tmed)CuCo$(CO)_4$, with some notable subtle differences. The coordination about the Cu atom is nearly planar with Cu, Co, C(13), N(1), and N(2) atoms defining the plane. The Cu–Co distance is 2.404 (1) Å, which is significantly longer than the corresponding parameter in (tmed)CuCo$(CO)_4$. Nevertheless, it is clearly within bonding distance and is shorter than would be

---

(6) Sheldrick, G. *SHELXTL-PLUS* revision 3.4; Nicolet Instrument Corp.: Madison, WI, 1988.

(7) Cromer, D. T.; Waber, J. T. *International Tables for X-ray Crystallography*; Kynoch Press: Birmingham, England, 1974; Vol. IV, pp 55, 99.

**Table III.** Bond Lengths (Å) and Bond Angles (deg) for (bpy)CuCo(CO)$_4$

| | | | |
|---|---|---|---|
| (a) Bond Lengths | | | |
| Cu–Co | 2.404 (1) | Cu–N(1) | 2.046 (3) |
| Cu–N(2) | 2.042 (3) | Cu–C(11) | 2.608 (4) |
| Cu–C(13) | 2.088 (4) | Co–C(11) | 1.778 (4) |
| Co–C(12) | 1.775 (4) | Co–C(13) | 1.788 (4) |
| Co–C(14) | 1.786 (4) | N(1)–C(1) | 1.351 (4) |
| N(1)–C(5) | 1.357 (4) | C(1)–C(2) | 1.382 (5) |
| C(2)–C(3) | 1.383 (5) | C(3)–C(4) | 1.381 (5) |
| C(4)–C(5) | 1.385 (4) | C(5)–C(6) | 1.493 (4) |
| C(6)–C(7) | 1.395 (5) | C(6)–N(2) | 1.345 (4) |
| C(7)–C(8) | 1.385 (5) | C(8)–C(9) | 1.380 (5) |
| C(9)–C(10) | 1.376 (5) | C(10)–N(2) | 1.345 (4) |
| C(11)–O(11) | 1.152 (5) | C(12)–O(12) | 1.139 (4) |
| C(13)–O(13) | 1.167 (5) | C(14)–O(14) | 1.132 (5) |
| (b) Bond Angles | | | |
| Co–Cu–N(1) | 130.1 (1) | Co–Cu–N(2) | 149.0 (1) |
| N(1)–Cu–N(2) | 81.0 (1) | Co–Cu–C(11) | 41.3 (1) |
| N(1)–Cu–C(11) | 94.5 (1) | N(2)–Cu–C(11) | 157.2 (1) |
| Co–Cu–C(13) | 46.2 (1) | N(1)–Cu–C(13) | 171.3 (1) |
| N(2)–Cu–C(13) | 103.0 (1) | C(11)–Cu–C(13) | 84.8 (1) |
| Cu–Co–C(11) | 75.5 (1) | Cu–Co–C(12) | 143.9 (1) |
| C(11)–Co–C(12) | 105.6 (2) | Cu–Co–C(13) | 57.5 (1) |
| C(11)–Co–C(13) | 126.9 (2) | C(12)–Co–C(13) | 99.6 (2) |
| Cu–Co–C(14) | 106.0 (1) | C(11)–Co–C(14) | 108.0 (2) |
| C(12)–Co–C(14) | 107.7 (2) | C(13)–Co–C(14) | 107.5 (2) |
| Cu–N(1)–C(1) | 128.3 (2) | Cu–N(1)–C(5) | 114.0 (2) |
| C(1)–N(1)–C(5) | 117.7 (3) | N(1)–C(1)–C(2) | 123.3 (3) |
| C(1)–C(2)–C(3) | 118.4 (3) | C(4)–C(3)–C(4) | 119.2 (3) |
| C(3)–C(4)–C(5) | 119.6 (3) | N(1)–C(5)–C(4) | 121.7 (3) |
| N(1)–C(5)–C(6) | 115.1 (3) | C(4)–C(5)–C(6) | 123.2 (3) |
| C(5)–C(6)–C(7) | 122.3 (3) | C(5)–C(6)–N(2) | 115.8 (3) |
| C(7)–C(6)–N(2) | 121.9 (3) | C(6)–C(7)–C(8) | 118.6 (3) |
| C(7)–C(8)–C(9) | 119.5 (3) | C(8)–C(9)–C(10) | 118.6 (3) |
| C(9)–C(10)–N(2) | 123.0 (3) | Cu–N(2)–C(6) | 114.1 (2) |
| Cu–N(2)–C(10) | 127.5 (2) | C(6)–N(2)–C(10) | 118.4 (3) |
| Cu–C(11)–Co | 63.2 (1) | Cu–C(11)–O(11) | 121.3 (2) |
| Co–C(11)–O(11) | 175.5 (3) | Co–C(12)–O(12) | 177.8 (3) |
| Cu–C(13)–Co | 76.3 (1) | Cu–C(13)–O(13) | 121.5 (3) |
| Co–C(13)–O(13) | 162.1 (3) | Co–C(14)–O(14) | 178.0 (3) |

**Table IV.** Comparison of Bond Angles (deg) and Bond Lengths (Å) between (tmed)CuCo(CO)$_4$ and (bpy)CuCo(CO)$_4$

| | (tmed)CuCo(CO)$_4$ | (bpy)CuCo(CO)$_4$ |
|---|---|---|
| Cu–Co | 2.379 (1) | 2.404 (1) |
| Cu–CO(bridging) | 2.032 (9) | 2.088 (4) |
| Co–CO(bridging) | 1.798 (9) | 1.788 (4) |
| Co–CO(terminal) | 1.760 (3) | 1.780 (4) |
| Cu–C–O(bridging) | 123.5 (7) | 121.5 (3) |
| Co–C–O(bridging) | 159 (1) | 162.1 (3) |

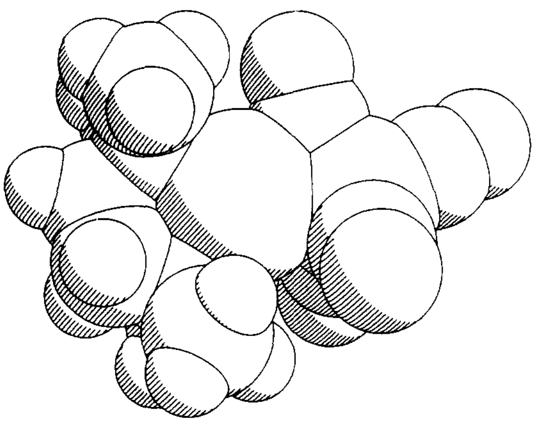

**Figure 3.** Space-filling diagram of (tmed)CuCo(CO)$_4$.

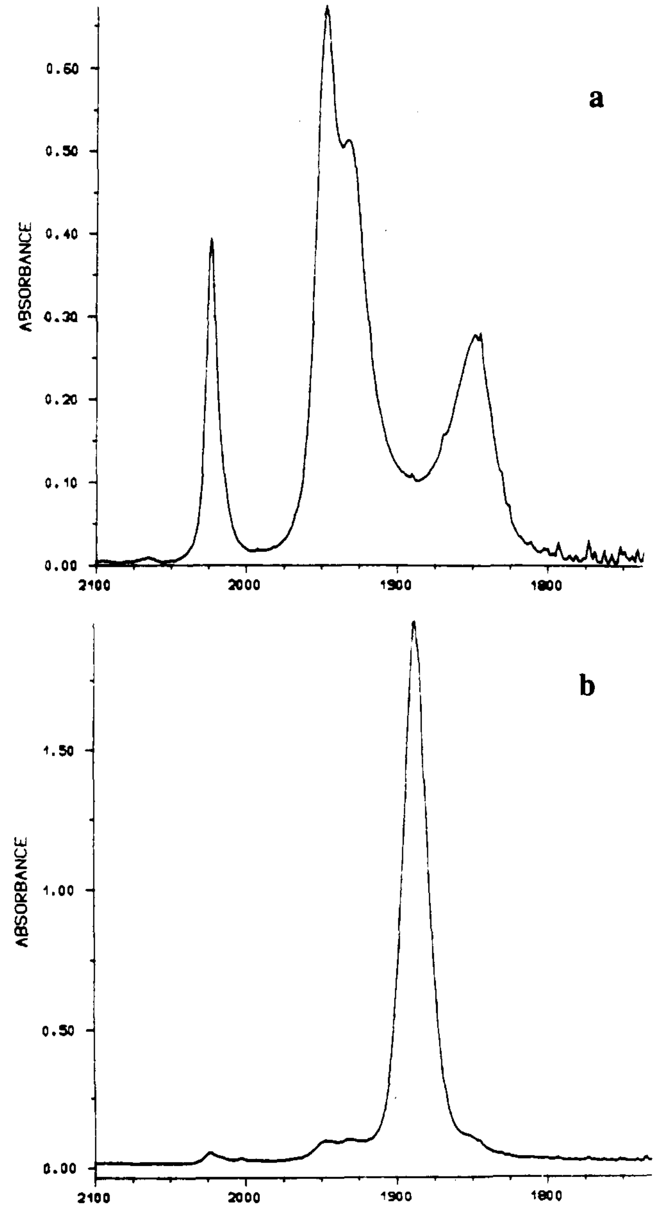

**Figure 4.** Infrared spectra in the $\nu$(CO) region of the reaction between (bpy)CuCo(CO)$_4$ and dppe (dppe = $Ph_2PCH_2CH_2PPh_2$) in THF at −78 °C: (a) initial spectrum of (bpy)CuCo(CO)$_4$; (b) spectrum after its conversion into Co(CO)$_4^-$ anion.

expected on the basis of Cu–Cu and Co–Co bond lengths observed in the metals (2.55 and 2.51 Å, respectively).[8] One of the carbonyl groups, C(13)–O(13), asymmetrically bridges the Cu–Co bond. Indeed, it is this strongly bridging CO ligand that is proposed to account for the short Cu–Co bond in (tmed)CuCo(CO)$_4$.[3] The Cu–C(13) distance is 2.088 (4) Å, which is considerably longer than that observed in terminal or bridging CO groups bonded directly to Cu(I). For example, terminal Cu–CO bond distances in the complexes [Cu(dien)CO]$^+$, [Cu$_2$(tmen)$_2$(CO)$_2$Cl]$^+$, and [Cu(2-Mequin)(CO)]$_4$ range in value from 1.76 to 1.79 Å,[9,11] whereas the bridging Cu–CO bond distance in [Cu$_2$(tmen)$_2$($\mu$-PhCO$_2$)($\mu$-CO)]$^+$ is 1.868 (8) Å.[12] On the other hand, the Co–C(13) bond length at 1.788 (4) Å is not significantly longer than the average terminal Co–C bond length of 1.780 (4) Å. The carbonyl group is bent away from the Cu atom with a Cu–C(13)–O(13) angle of 121.5 (3)° and a Co–C(13)–O(13) angle of 162.1 (3)°. Table IV lists a comparison of bond angles and

---

(8) Pauling, L. In *The Nature of the Chemical Bond*, 3rd ed.; Cornell University Press: Ithaca, NY, 1960; p 410.

(9) Pasquali, M.; Marchetti, F.; Floriani, C. *Inorg. Chem.* **1978**, *17*, 1684.

(10) Pasquali, M.; Floriani, C.; Gaetani-Manfredotti, A. *Inorg. Chem.* **1981**, *20*, 3382.

(11) Floriani, C.; Chiesi-Villa, A.; Guastini, C.; Zanazzi, P. F. *J. Chem. Soc., Dalton Trans.* **1988**, 1607.

(12) Pasquali, M.; Floriani, C.; Venturi, G.; Gaetani-Manfredotti, A.; Chiesi-Villa, A. *J. Am. Chem. Soc.* **1982**, *104*, 4092.

bond lengths in (tmed)CuCo$(CO)_4$ and (bpy)CuCo$(CO)_4$.

The longer Cu–Co bond length in the 2,2′-bipyridine derivative as compared to that in the tetramethylethylenediamine derivative is reflected in a longer, and presumably weaker, Cu-bridging CO bond in the former species. This observation is consistent with the lower $\nu$(CO) vibration seen in the solid-state infrared spectrum for the semibridging CO ligand (1820 cm$^{-1}$) in (tmed)CuCo$(CO)_4$ as compared to the analogous vibration in (bpy)CuCo$(CO)_4$ at 1850 cm$^{-1}$. It is most interesting however that while (bpy)CuCo$(CO)_4$ exhibits a low-frequency $\nu$(CO) mode at 1850 cm$^{-1}$ in both the solid state and THF solution, the (tmed)CuCo$(CO)_4$ derivative's bridging $\nu$(CO) vibration shifts from 1820 cm$^{-1}$ in the solid state to 1860 cm$^{-1}$ in $CH_2Cl_2$ solution.

On the basis of the shift of the bridging $\nu$(CO) in (tmed)CuCo$(CO)_4$ from 1820 cm$^{-1}$ in the solid state to 1860 cm$^{-1}$ in solution, it has been suggested that there is disruption of the semibridging CO ligand in solution as a result of solvent coordination to the copper center.[2,3] However, the solution-phase $\nu$(CO) frequency for this derivative at 1860 cm$^{-1}$ is quite similar to that observed herein for the analogous (bpy)CuCo$(CO)_4$ complex, where a semibridging CO moiety is clearly present. Hence, we conclude that the bridging CO ligand in (tmed)CuCo$(CO)_4$ is less associated with the copper center in solution than in the solid state. Nevertheless, it is still bridging the two metal centers asymmetrically. The solution structure may be the result of a 90° rotation about the Cu–Co bond, leading to a more normal Cu(I) tetrahedral arrangement of ligands.[13]

It is apparent from a comparison of the space-filling models of the (bpy)CuCo$(CO)_4$ and (tmed)CuCo$(CO)_4$ derivatives (Figures 2 and 3) that there is no hindrance to solvent coordination at the copper center of either derivative. Yet in the bpy complex no shift in the bridging $\nu$(CO) vibration is noted in going from the solid state to the very polar THF solution. The reason for this difference in behavior of the two bimetallic derivatives is not clear. On the other hand, use of the highly coordinating dppe ligand rapidly cleaves the Cu–Co bond in both derivatives at −78 °C in THF with concomitant formation of $Co(CO)_4^-$. For example, the infrared spectrum in the $\nu$(CO) region of (bpy)CuCo$(CO)_4$ in THF is characterized by four bands at 2024 (s), 1947 (s), 1932 (2, sh), and 1850 (m) cm$^{-1}$. The formation of the $Co(CO)_4^-$ anion was judged by the appearance of its diagnostic $\nu$(CO) band at 1886 cm$^{-1}$. The infrared spectra for this process are depicted in Figure 4. On the other hand, the infrared spectrum of (bpy)CuCo$(CO)_4$ was not altered in refluxing THF over a 24-h period. Both (bpy)CuCo$(CO)_4$ and (tmed)CuCo$(CO)_4$ are insoluble in, and unreactive toward, deoxygenated water. This was demonstrated by the lack of detection of $Co(CO)_4^-$ in water by infrared spectroscopy, with the complexes being recovered unaltered.

**Acknowledgment.** The financial support of this research by the National Science Foundation (Grant CHE 88-17873) and the Robert A. Welch Foundation is greatly appreciated.

**Supplementary Material Available:** Tables of hydrogen atom coordinates, anisotropic thermal parameters, and crystal data and data collection parameters for (bpy)CuCo$(CO)_4$ (4 pages); a table of calculated and observed structure factors (9 pages). Ordering information is given on any current masthead page.

(13) This was suggested by an anonymous reviewer of this paper.

---

Contribution from the Department of Chemistry,
Washington University, St. Louis, Missouri 63130

# Preparation of Six Lead(II) Dialkoxides, X-ray Crystal Structures of $[Pb(\mu,\eta^1\text{-}OCH_2CH_2OMe)_2]_\infty$ and $[Pb_3(\mu\text{-}O\text{-}t\text{-}Bu)_6]$, and Hydrolysis Studies

Subhash C. Goel, Michael Y. Chiang, and William E. Buhro*

*Received October 30, 1989*

Six lead(II) dialkoxides prepared by alcoholyses of $Pb[N(SiMe_3)_2]_2$ are described: Pb(O-*i*-Pr)$_2$ (**1**), Pb(O-*t*-Bu)$_2$ (**2**), $Pb(OCMe_2Et)_2$ (**3**), $Pb(OCEt_3)_2$ (**4**), $Pb(OCH_2CH_2OMe)_2$ (**5**), and $Pb(OCHMeCH_2NMe_2)_2$ (**6**). All except **1** and **5** have good solubility in organic solvents. The compounds sublime or distill in the range 95–170 °C at $10^{-4}$ Torr; only **5** decomposes during sublimation. Hydrolysis of **3** or **6** in THF gives $3PbO\cdot H_2O$, which is not converted to massicot or litharge (polymorphs of PbO) by refluxing the reaction slurry. However, the first-formed $3PbO\cdot H_2O$ is converted to litharge when **3** is hydrolyzed in the presence of 10 mol % of $LiOCMe_2Et$ and the resulting slurry is refluxed. Two compounds are completely structurally characterized: $[Pb(\mu,\eta^1\text{-}OCH_2CH_2OMe)_2]_\infty$ (**5**) and $[Pb_3(\mu\text{-}O\text{-}t\text{-}Bu)_6]$ (**2**). Compounds **5** and **1** are isostructural in the solid state. Crystal data for **5**: monoclinic, $C2/c$, $a = 11.411$ (8) Å, $b = 14.641$ (6) Å, $c = 6.278$ (3) Å, $\beta = 108.34$ (5)°, $V = 995.6$ (9) Å$^3$, $T = 22$ °C, $Z = 4$, and $D_c = 2.384$ g cm$^{-3}$. Of the 3794 intensities measured, 1026 unique reflections with $I > 3\sigma(I)$ yielded $R(F_o) = 0.0258$ and $R_w(F_o) = 0.0320$. Crystal data for **2**: trigonal (hexagonal axes), $R\bar{3}$, $a = b = 10.174$ (2) Å, $c = 29.491$ (9) Å, $V = 2643.6$ (11) Å$^3$, $T = 22$ °C, $Z = 3$, and $D_c = 1.998$ g cm$^{-3}$. Of the 1566 intensities measured, 517 unique reflections with $I > 3\sigma(I)$ yielded $R(F_o) = 0.0504$ and $R_w(F_o) = 0.0592$.

## Introduction

We are interested in lead(II) dialkoxides as potential precursors[1] for vapor- and solution-phase syntheses of lead-substituted oxide superconductors[2] and lead-containing oxide ceramics in general.[3] There are a few reports of the in situ generation of lead(II) alkoxides in preparations of oxide ceramics,[4–7] but in none of these

---

(1) (a) Hubert-Pfalzgraf, L. G. *New J. Chem.* **1987**, *11*, 663. (b) Livage, J.; Henry, M.; Sanchez, C. *Prog. Solid State Chem.* **1988**, *18*, 259. (c) Bradley, D. C. *Chem. Rev.* **1989**, *89*, 1317.

(2) Sunshine, S. A.; Siegrist, T.; Schneemeyer, L. F.; Murphy, D. W.; Cava, R. J.; Batlogg, B.; van Dover, R. B.; Fleming, R. M.; Glarum, S. H.; Nakahara, S.; Farrow, R.; Krajewski, J. J.; Zajurak, S. M.; Waszczak, J. V.; Marshall, J. H.; Marsh, P.; Rupp, L. W., Jr.; Peck, W. F. *Phys. Rev. B* **1988**, *38*, 893.

(3) (a) Heartling, G. H.; Land, C. E. *J. Am. Ceram. Soc.* **1971**, *54*, 1. (b) Lipeles, R. A.; Coleman, D. J.; Leung, M. S. In *Better Ceramics Through Chemistry II*; Brinker, C. J., Clark, D. E., Ulrich, D. R., Eds.; MRS Proceedings, Vol. 73; Materials Research Society: Pittsburgh, PA, 1986; pp 665–670. (c) Budd, K. D.; Dey, S. K.; Payne, D. A. *Ibid.*, pp 711–716.

(4) Brown, L. M.; Mazdiyasni, K. S. *J. Am. Ceram. Soc.* **1972**, *55*, 541.

(5) Yamaguchi, O.; Yamadera, M.; Shimizu, K. *J. Am. Ceram. Soc.* **1977**, *50*, 2805.

(6) Narita, E.; Kobayashi, M.; Shinjo, H.; Tsuchida, H. *Bull. Chem. Soc. Jpn.* **1983**, *56*, 3129.